

See discussions, stats, and author profiles for this publication at: <https://www.researchgate.net/publication/6633829>

Fast Processes and Intermediates in Photochemistry of 7-Dimethyl-germanorbornadiene

ARTICLE *in* THE JOURNAL OF PHYSICAL CHEMISTRY A · JANUARY 2007

Impact Factor: 2.69 · DOI: 10.1021/jp0604950 · Source: PubMed

CITATIONS

5

READS

51

5 AUTHORS, INCLUDING:



Victor F Plyusnin

Institute of Chemical Kinetics and Combustion ...

163 PUBLICATIONS **1,154** CITATIONS

SEE PROFILE



Tatyana Leshina

Institute of Chemical Kinetics and Combustio...

126 PUBLICATIONS **1,195** CITATIONS

SEE PROFILE

ARTICLES

Fast Processes and Intermediates in Photochemistry of 7-Dimethyl-germanorbornadiene

Margarita V. Kaletina, Victor F. Plyusnin,* Vyacheslav P. Grivin, Valeriy V. Korolev, and Tatyana V. Leshina

*Institute of Chemical Kinetics and Combustion SB RAS, 630090, Novosibirsk, Russia**Received: January 24, 2006; In Final Form: October 9, 2006*

Laser pulse photolysis experiments have shown that the triplet excited-state of 1,2,3,4-tetraphenylnaphthalene (TPN) is one of the primary intermediates of the photochemical transformation of 7,7'-dimethylgerma-1,4,5,6-tetraphenyl-2,3-benzo-norbornadiene (GNB) in hexane solution. The molar absorption of T–T absorption and the quantum yield of the intersystem crossing of TPN were determined from the triplet–triplet energy transfer. The scheme of GNB photocleavage has been suggested where the triplet excited TPN originated from the triplet state of biradical through cleavage of the second C–Ge bond, the latter being generated from the excited singlet state of the initial GNB after the cleavage of the first C–Ge bond and the intersystem crossing. Other channels of GNB's chemical transformation have been discussed.

1. Introduction

Germynes are known to be reactive intermediates in the chemical and photochemical transformations of many germanium-containing compounds.^{1–8} Most papers in this area are devoted to the spectroscopy of dimethylgermylene (Me_2Ge) and the kinetics of its transformations.^{3–5,7–14} 7,7'-Dimethylgerma-1,4,5,6-tetraphenyl-2,3-benzo-norbornadiene (GNB) is a convenient source of Me_2Ge ; by exposing GNB to high temperatures or UV-irradiation, it decomposes into Me_2Ge and 1,2,3,4-tetraphenylnaphthalene (TPN).^{2,15–19} However, data on the elementary stages of the photochemical transformations of GNB are rather contradictory. Therefore, an application of the ^1H CIDNP method suggests two different pathways of GNB phototransformation.^{20–22} The first pathway involves a one-step mechanism of GNB dissociation, accompanied by the simultaneous cleavage of both Ge–C bonds. The second pathway is a two-step mechanism of GNB photocleavage through the consecutive cleavage of two Ge–C bonds.^{21,22} According to these suggestions, the cleavage of one of the Ge–C bonds in the excited singlet state of GNB results in a biradical in the singlet state, which could recombine and/or undergo the

intersystem crossing into the triplet state. The cleavage of the second Ge–C bond occurs in the triplet biradical that, in turn, leads to the formation of triplet dimethylgermylene and TPN in the singlet ground state (note that the suggested scheme does not exclude another way for the transformation of the triplet biradical or the formation of TPN in an excited triplet state and dimethylgermylene in a singlet ground state).

There have been other attempts to use laser pulse photolysis to detect the intermediates in GNB photocleavage.²⁰ These studies showed that the excitation of GNB results in formation of TPN in the excited triplet state. GNB is assumed²⁰ to dissociate in synchronous breaking of both Ge–C bonds over a picosecond time scale. In this case, TPN is formed in the singlet excited state and rapidly converts to the triplet state. Because no spectroscopic manifestations of Me_2Ge were observed, it was concluded that this particle rapidly (hundreds of nanoseconds) dimerizes into tetramethyldigermene. However, this rapid recombination requires high Me_2Ge concentrations ($\geq 10^{-3}$ M), exceeding the initial GNB concentration. It is worth noting that even at 77 K no intermediates were recorded in the frozen matrix of methylcyclohexane, despite a high quantum yield ($\phi = 0.37$) of GNB dissociation. Unfortunately, the molar

absorption of triplet–triplet (T–T) absorption was not measured,²⁰ and a relative yield of the triplet TPN state remains unknown. Therefore, it could be possible that the formation of TPN in the triplet state is not the main channel of GNB photodissociation. In addition, the initial GNB may contain residual TPN as an impurity. In the UV region, the TPN molecule has a stronger absorption than GNB. Therefore, laser pulse photolysis experiments could easily observe T–T absorption as a result of direct excitation of TPN.

In the present work, we revised earlier suggested schemes of GNB phototransformations by means of comprehensive analysis of all sources of formation of TPN in triplet state. We have measured the molar absorption of TPN T–T absorption using the energy transfer to anthracene to determine the contribution of the channel of GNB photodissociation resulting in the tetraphenylanthracene molecule in the triplet state. We have also carefully analyzed the dynamics of the intermediate absorption to demonstrate that it is observed on a nanosecond time scale, which differs from the T–T absorption and can belong to both biradical and dimethylgermylene.

2. Experimental Section

Laser pulse photolysis setup with an excimer XeCl laser (308 nm), pulse duration of 15 ns and a mean energy pulse of 20 mJ has been used.²³ Exciting and probing beams intersect at a small angle ($\sim 2^\circ$) in a sample. All measurements were performed in a cell with an optical path length of 1 cm. For stationary photolysis, we employed irradiation of either the XeCl laser or mercury lamp (DRSh –500) with a set of glass filters to isolate single lines. Optical absorption spectra were recorded using an HP 8453 diode array spectrophotometer. Spectrally pure hexane (Merck) was used for preparation of solutions. All measurements were carried out in the absence of oxygen, which was removed by purging the solutions with argon for 20 min (the residual concentration of oxygen was estimated from the kinetics of anthracene T–T absorption decay and it was below 1.5×10^{-6} M). The standard GNB concentration was about 1×10^{-4} M, which corresponded to the optical densities of the solution at a laser wavelength (308 nm) on the order of 0.1–0.2.

GNB was synthesized as previously described.¹⁹ The amount of TPN impurity in GNB samples was determined by measuring luminescence intensity. The TPN molecule in methylcyclohexane and ethanol exhibits a fluorescence band with a maximum at 360 nm, a quantum yield of 0.09 and a lifetime of 2.9–3.2 ns.²⁰ The fresh GNB in solutions has shown a very weak luminescence. Therefore, the values of fluorescence intensity before irradiation and after the complete phototransformation of GNB to TPN under UV irradiation were used to estimate the amount of TPN additive in the GNB preparation. These measurements indicate that the impurity of TPN in our preparation was about $3.5 \pm 0.5\%$, and its presence was taken into account when further processing the results of laser pulse photolysis measurements.

The absorption coefficient of TPN T–T absorption was determined from the data on energy transfer between the triplet levels of TPN and anthracene (ANT). Laser pulse intensity in sample cell was estimated from the optical density of triplet–triplet absorption of anthracene in oxygen-free benzene solution at 431 nm (the quantum yield of the triplet state is 0.53, the molar absorption coefficient of T–T absorption band is $42\,000\text{ M}^{-1}\text{cm}^{-1}$).²⁴ Numerical modeling of the kinetics for the decay of transient optical absorption involved the solution of corresponding differential equations by means of an in-house program based on the Runge–Kutta method of the fourth order.

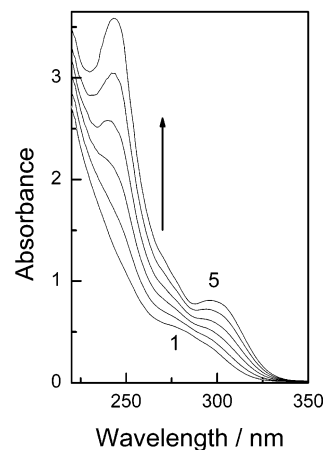


Figure 1. Change in the optical spectrum of GNB (1.37×10^{-4} M) in hexane under irradiation with XeCl laser pulses (308 nm, energy 20 mJ for 3 mL of solution and intensity $0.15\text{ J}\cdot\text{cm}^{-2}$ per pulse). For 1–5: 0, 5, 15, 30, 60, and 230 pulses, respectively.

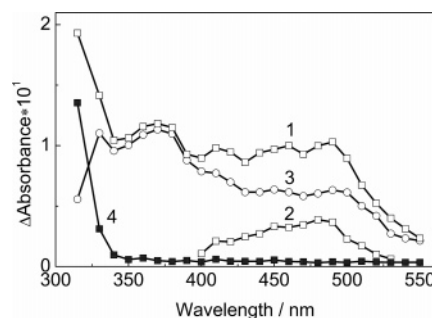


Figure 2. Spectrum of transient absorption generated in the pulse photolysis of GNB (1.0×10^{-4} M) in hexane. 1: the absorption formed after laser pulse (50 ns); 2–4: the spectra of rapid A_1 components, slow A_2 components, and $\Delta D(\infty)$, respectively (the processing of the kinetic curves according to eq 1).

3. Results and Discussion

3.1. Stationary Photolysis of GNB Solution. Figure 1 shows a change in optical spectrum under stationary irradiation of GNB solution in hexane. The coefficients of TPN absorption in hexane are $\epsilon^{308} = 9600$ and $\epsilon^{242} = 51\,500\text{ M}^{-1}\text{cm}^{-1}$, which almost coincide with values in benzene.²⁰ The initial GNB has a weaker absorption ($\epsilon^{308} = 1600$ and $\epsilon^{242} = 13\,700\text{ M}^{-1}\text{cm}^{-1}$). Therefore, under irradiation, the kinetic curves are rapidly saturated due to laser light absorption by TPN molecules. For example, the last spectrum in Figure 1 corresponds to the transformation of about 60% of GNB to TPN. The quantum yield of GNB photodissociation under irradiation at 308 nm measured by the initial angle of kinetic curves was $\varphi = 0.31$, which is in fair agreement with the values of quantum yield presented in previous studies.²⁰ The final spectrum fully coincides with the GNB (40%) and TPN (60%) spectra. Thus, the germanium-containing products of GNB photodissociation show weaker absorption as compared with that of TPN.

3.2. Laser Pulse Photolysis of GNB Solution. The spectrum of transient absorption that arises after a laser pulse in hexane fresh GNB solution is shown in Figure 2. The kinetic curves at the selected wavelengths are given in Figure 3. In the UV region ($\lambda < 340\text{ nm}$), 10–15 μs after the pulse, the absorption remains constant and is attributed to TPN. It is worth noting that the initial slope of the kinetic curves depends on the spectral range of recording, which is evident from the kinetic curves (Figure 3). This indicates that the laser pulse gives rise to two intermediates that disappear at quite different rates.

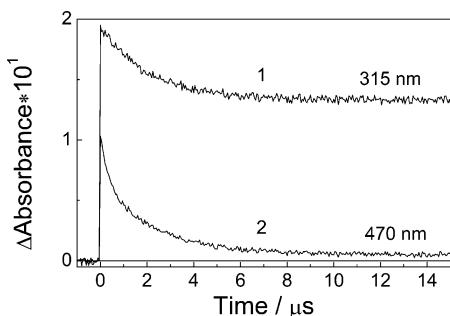


Figure 3. Kinetic traces of a change in transient absorption generated in the pulse photolysis of GNB (1.0×10^{-4} M) in hexane. 1 and 2: recording wavelengths 315 and 470 nm, respectively.

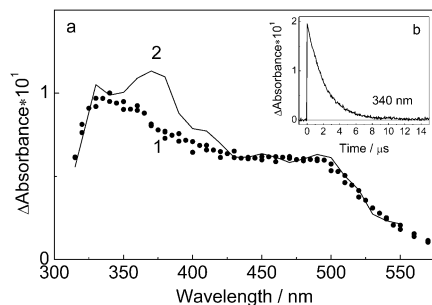


Figure 4. Spectra (a) of the triplet–triplet absorption of TPN (1) and the slow A_2 component (2) absorption in hexane. (b) The decay kinetics of TPN T–T absorption.

To distinguish the spectra of these particles, the kinetic curves ($\Delta D(t)$) are treated in the framework of the two-exponential model

$$\Delta D(t) = A_1 e^{-k_1 t} + A_2 e^{-k_2 t} + \Delta D(\infty) \quad (1)$$

where A_1 and A_2 are the optical densities of the absorption of the particles disappearing with the rate constants k_1 and k_2 , respectively, and $\Delta D(\infty)$ is the optical density at long times after the pulse, which is actually the TPN spectrum. Figure 2 shows the spectra of components A_1 and A_2 , that is, the spectra of two particles. The spectrum of the slow component (A_2) covers a wide spectral range from 300 to 600 nm. The decay rate constant is $(4.6 \pm 0.6) \times 10^5 \text{ s}^{-1}$, that is, this particle disappears within about 2 μs . A fast component is localized in a more narrow spectral range from 400 to 550 nm, and its decay rate constant is $(3.3 \pm 0.4) \times 10^6 \text{ s}^{-1}$ (~ 300 ns).

It is known that the addition of two phenyl groups (diphenyl-naphthalene molecule) widens the narrow bands of T–T absorption of naphthalene²⁵ and shifts the spectrum from a range of 415–430 nm to 480–500 nm.²⁶ The existence of four phenyl groups in TPN could lead to the formation of structureless T–T absorption over a wide spectral range. Thus, the spectrum of the slow component can be assigned to the appearance of TPN T–T absorption. This can be verified by recording the spectrum of transient absorption during laser pulse photolysis of TPN in hexane (Figure 4). The TPN T–T and slow (A_2) component absorption spectra normalize at 450 nm, which coincide with each other, except for the 340–420 nm spectral region, where an additional band with a maximum of 370 nm is present for A_2 (Figure 4). While processing the kinetic curves for TPN in hexane, it was observed that in these two cases, the rate constants of absorption decay coincide. The nature of 370 nm additional band for A_2 will be discussed later.

In previous studies²⁰ of GNB photochemistry, the intermediate absorption is assigned only to the triplet TPN state, which, in

TABLE 1: Spectroscopic Characteristics of Dimethylgermylene in 3-MP Frozen Matrices (77 K) and Cyclohexane Solutions (300 K)

precursor	λ (nm)		
	77 K	300 K	ref
$\text{Me}_2\text{Ge}(\text{N}_3)_2$	405 (Ar, 26 K)		9
$\text{PhGeMe}_2(\text{SiMe}_3)$	418	425	8
Me_2GeNB	420		11, 12
$\text{Me}_2\text{Ge}(\text{SePh})_2$	420	420	10
$(\text{PhMe}_2\text{Ge})_2\text{GeMe}_2$	422		7
$(\text{PhMe}_2\text{Ge})_2\text{GeMe}_2$	422	420	3, 4
Dinezo-1,1',2,2',3,3'-hexamethyl-1,2,3-trigermacyclohepta-4,6-diene	430		13
$[\text{Me}_2\text{Ge}]_6$	430	450	5
$\text{PhMe}_2\text{Ge}-\text{GeMe}_3$		430	28
$[\text{Me}_2\text{Ge}]_6$	430		7
$\text{Me}[\text{Me}_2\text{Ge}]_5\text{Me}$	436		7
$(\text{PhMe}_2\text{Ge})_2$		440	29
PMDGeN		440	30
$[\text{Me}_2\text{Ge}]_5$	506	490	14

the absence of oxygen, disappears within some microseconds. However, from the two presented kinetics in this paper,²⁰ it could be concluded that the observed rate constant (k_{obs}) of absorption decay at 480 nm is substantially higher (at least two times) than the rate constant at 310 nm. Thus, the kinetic curves at various wavelengths have not been carefully analyzed,²⁰ and the fast component (A_1) was not detected. Dimethylgermylene is likely to be an active intermediate, which could be assigned to the fast component (A_1). This data could be examined using $\text{Me}_2\text{-Ge}$ spectroscopy in frozen matrices and solutions.

3.3. Dimethylgermylene Spectroscopy in Frozen Matrices and Solutions. The photolysis of GNB in frozen 3-methylpentane (3-MP) glasses (77 K) leads to the appearance of optical absorption bands with maxima at 420 and 317 nm.^{11,12} The first band disappears at the temperatures exceeding that of the matrix melting point and was attributed to dimethylgermylene. The second band, which is still observed in the spectrum after the sample annealing, was attributed to TPN. The positions of $\text{Me}_2\text{-Ge}$ bands observed for other precursors are shown in Table 1.

The photolysis of GNB in the frozen matrix of toluene- d_8 leads to the appearance of an absorption band with a maximum at 420 nm,²⁷ similar to the photolysis of many other germanium-containing compounds (Table 1). However, as opposed to all other papers, some studies²⁷ have assigned this band not to dimethylgermylene, but to a biradical arising from the cleavage of only one Ge–C bond ($\text{TPN}^{\bullet}-\bullet\text{GeMe}_2$). This assumption is corroborated by the absence of a noticeable decomposition of germanorbornadiene after the annealing of the irradiated matrix. It was assumed that upon heating the matrix, the homolysis of the second Ge–C bond is much slower than the recombination of the first bond. At higher temperatures, the rate constant of the second bond homolysis could increase faster than the recombination rate constant. According to these studies,²⁷ the latter explains the decomposition of GNB under UV irradiation in solution.

Germylene is formed through the photodissociation of many germanium-containing compounds. For example, laser pulse photolysis of aryl-substituted trigermanes ($\text{R}^1_3\text{Ge}-\text{Ge}(\text{R}_2\text{R}_3)-\text{GeR}^1_3$) demonstrates the appearance of germylene absorption bands with maxima in the range of 420–450 nm after the pulse.^{3,4} Laser pulse photolysis (fourth harmonic of Nd laser at 266 nm) of 12-methyl-cyclohexagermane ($(\text{Me}_2\text{Ge})_6$) in cyclohexane⁵ results in the absorption band of dimethylgermylene with a maximum at 450 nm. The decay of this band in the second-order reaction ($2k/\epsilon = 2.7 \times 10^7 \text{ cm s}^{-1}$, where $2k$ is the rate constant of recombination and ϵ is molar absorption

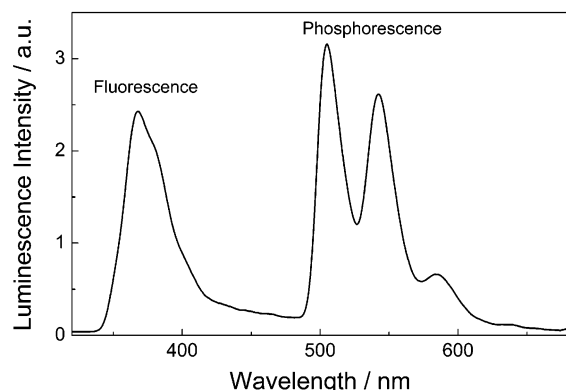


Figure 5. Fluorescence and phosphorescence spectra of TPN in methylcyclohexane matrix at 77 K.

coefficient of dimethylgermylene) is followed by the appearance of a new band at 370 nm belonging to tetramethylgermane ((Me₂Ge)₂).

Excitation (266 nm) of 10-methyl-cyclopentagermane ((Me₂-Ge)₅) in cyclohexane¹⁴ results in the formation of a particle with an absorption band at 490 nm immediately after the laser pulse, which disappears through recombination ($2k/\epsilon = 3.5 \times 10^7 \text{ cm s}^{-1}$). In this case, a new band is formed with a maximum at 370 nm, which disappears in the second-order reaction. The first band belongs to dimethylgermylene, and the second band belongs to the product of its dimerization, that is, tetramethyldigermene ((Me₂Ge)₂). Laser pulse photolysis (266 nm) of phenyl bis(trimethyl-silyl)germane (PhGeMe₂SiMe₃) in cyclohexane leads to the appearance of a wide absorption band with a maximum at 425 nm, which was attributed to dimethylgermylene.⁸ A similar absorption band with a maximum at 420 nm arises after the laser pulse (308 nm) in cyclohexane solution of dimethyl bis-(phenylseleno)germane (Me₂Ge(SePh)₂).¹⁰ Table 1 also summarizes the data on the location of the Me₂Ge absorption band maxima detected by pulse photolysis of different precursors. It is worth noting that even in the same solvent, the position of the band could move by as much as 30 nm to the extent that the generation of dimethylgermylene is carried out using various precursors.

Thus, Table 1 demonstrates a wide range of positions of the Me₂Ge absorption band maximum in a frozen matrix and in solutions when generated from various precursors. The band shift could be due to the different geometries (C–Ge–C angle) of dimethylgermylene present in the frozen matrix, when generated from various precursors. In solutions, this shift might occur due to the weak complexes formed from germylene interacting with the solvent.

In most cases, Me₂Ge disappears in the reaction of dimerization, resulting in tetramethyldigermene. The value of $2k/\epsilon \sim (1-5) \times 10^7 \text{ cm s}^{-1}$ points to a rather high recombination rate constant.^{5,8,10,14} Therefore, the additional absorption band with a maximum at 370 nm in the spectrum of the A₂ component detected (Figure 4) could be attributed to tetramethyldigermene ((Me₂Ge)₂) formed from the Me₂Ge recombination.

3.4. Molar Absorption Coefficient and Quantum Yield of the T–T Absorption of TPN. A relative yield of the triplet state of TPN in the GNB photodissociation can be determined using the absorption coefficient of TPN T–T absorption measured in the process of triplet–triplet energy transfer. Figure 5 shows the TPN luminescence spectrum in a methylcyclohexane matrix at 77 K. The band at 368 nm is associated with the fluorescence, and the other three bands with maxima at 505, 543, and 584 nm resulted from the phosphorescence of the triplet

TABLE 2: Quantum Yield and Spectroscopic Parameters of the Triplet State of Anthracene

solvent	φ_T	λ_T^{max} (nm)	ϵ_T (M ⁻¹ cm ⁻¹)	ref
benzene	0.53	430	42 000	24
benzene	0.5	430	45 500	33
cyclohexane	0.7	422	64 700	33
ethanol	0.58	424		34
toluene		428	42 000	35

level. Three bands correspond to the transitions from the zero vibronic level of the T₁ state to the vibronic levels with vibronic numbers 0, 1, and 2 of the ground S₀ state, respectively. The position of the first band determines the triplet level energy for TPN, $E_T = 2.45 \text{ eV}$ (note that for naphthalene $E_T = 3.15 \text{ eV}$ ³¹). Anthracene, with a much lower triplet level energy ($E_T = 1.82-1.89 \text{ eV}$),^{31,32} was used as an energy acceptor. The spectrum of the triplet–triplet absorption of anthracene in hexane consists of a strong and narrow band with a maximum at 421 nm, which actually coincides with the position of this band in cyclohexane, toluene,³³ and ethanol.³⁴ The absorption coefficients of this band are summarized in Table 2.

Processing of the kinetic curves of the T–T absorption decay indicates that the triplet state of anthracene in hexane at room temperature disappears through the first- and second-order reactions ($k_{1\text{ANT}} = (3.0 \pm 0.2) \times 10^4 \text{ s}^{-1}$ and $k_{2\text{ANT}} = (5.0 \pm 0.8) \times 10^9 \text{ M}^{-1}\text{s}^{-1}$, respectively). The second-order reaction is the reaction of triplet–triplet annihilation. The triplet–triplet TPN absorption in hexane disappears in the first-order reaction, with the rate constant $k_{1\text{TPN}} = (3.5 \pm 0.5) \times 10^5 \text{ s}^{-1}$. The kinetics of T–T absorption disappearance for TPN and anthracene are shown in Figure 6a (kinetics traces 2 and 3).

In a solution that contains TPN and anthracene, the total absorption of the triplet states of TPN and anthracene (ANT) arises just after the laser pulse because both of the molecules absorb at the wavelength of laser irradiation (308 nm). The

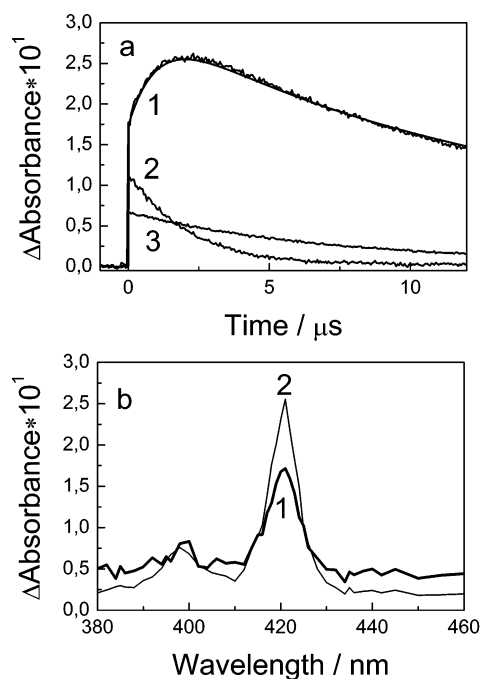


Figure 6. Kinetic traces (a) and spectra (b) of transient absorption arising at pulse photolysis of TPN ($1.0 \times 10^{-4} \text{ M}$) and ANT ($1.0 \times 10^{-4} \text{ M}$) solutions in hexane. (a) 1: The kinetic trace for TPN and ANT mixture. 2 and 3: The kinetic traces of T–T absorption decay of TPN and ANT in separate solutions. (b) 1 and 2: The spectra at 0 and 2 μs after laser pulse, respectively, for TPN and ANT mixture.

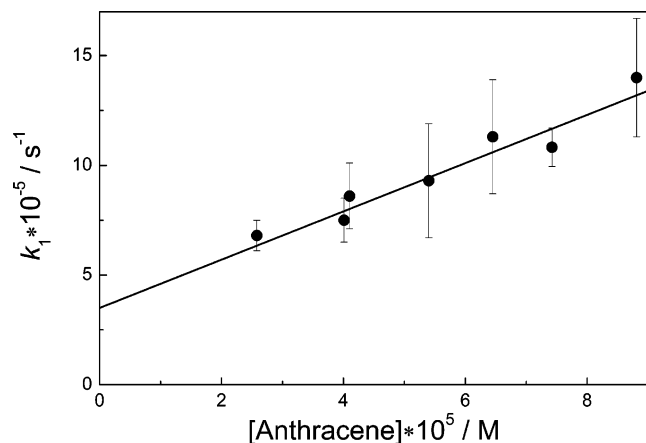


Figure 7. Dependence of the rate constant k_1 (fast exponent in eq 3) on anthracene concentration.

optical density in a maximum of the triplet anthracene absorption band (421 nm) increases over $\sim 2 \mu\text{s}$ as a result of energy transfer (kinetic curve 1 in Figure 6a).



Figure 6b shows both a change of the spectrum upon energy transfer and an increase in the triplet anthracene absorption band intensity at 421 nm. To determine the absorption coefficients of TPN T–T absorption, experiments were carried out at low intensities of the laser pulse when the concentrations of triplet molecules are small ($\sim 10^{-6} - 10^{-7} \text{ M}$), and the second-order reaction of anthracene in triplet state fails to contribute substantially to the kinetics of absorption disappearance. The kinetic curves at 421 nm were treated using the two-exponential approximation

$$\Delta D(t) = -A_1 e^{-k_1 t} + A_2 e^{-k_2 t} \quad (3)$$

where A_1 is the amplitude of the optical density increase due to energy transfer and A_2 is the absorption of anthracene in triplet state that results from both the direct excitation of anthracene ($\epsilon(308 \text{ nm}) = 1030 \text{ M}^{-1}\text{cm}^{-1}$) and the energy transfer (just after pulse, the absorption $A_0 = A_2 - A_1$). The rate constants in eq 3 at small signal amplitudes are of the form

$$k_1 = k_{1\text{TPN}} + k_{\text{TE}}[\text{ANT}], \quad k_2 = k_{1\text{ANT}} \quad (4)$$

where k_{TE} is the energy transfer rate constant. Figure 7 shows the dependence of k_1 on anthracene concentration whose slope determines the value $k_{\text{TE}} = (1.1 \pm 0.3) \times 10^{10} \text{ M}^{-1}\text{s}^{-1}$. This rate constant is close to the diffusion limit and enables energy transfer to successfully compete with the process of the deactivation of the TPN triplet state. Kinetics calculated with the parameters obtained (molar absorption coefficients and rate constants) are in fair agreement with the experimental kinetic curves (smooth curve 1 in Figure 6a).

The ratio between the absorption coefficients of the T–T absorption of TPN and anthracene at low intensities of the laser pulse can be written as follow:

$$\frac{\epsilon_{\text{ANT}}}{\epsilon_{\text{TPN}}} = \frac{k_{\text{TE}}[\text{ANT}]}{k_{1\text{TPN}} + k_{\text{TE}}[\text{ANT}]} \times \frac{A_2 - A_{0\text{ANT}}}{A_0 - A_{0\text{ANT}}} \quad (5)$$

where $A_{0\text{ANT}}$ is the contribution to the intermediate absorption due to direct anthracene excitation to triplet state calculated from the investigation of the pulse photolysis of only anthracene solutions. For solutions containing TPN and anthracene, $A_{0\text{ANT}}$

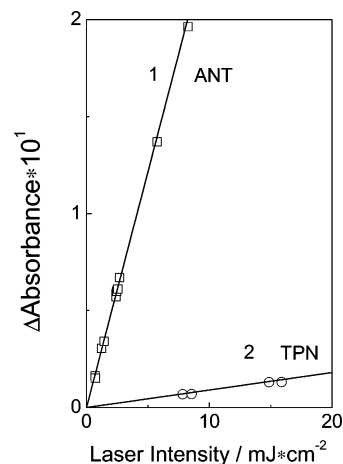


Figure 8. Dependence of the optical density of the T–T absorption of anthracene (1) and TPN (2) at 421 nm in hexane on laser pulse intensity

was calculated with regard to a fraction of the laser pulse quanta absorbed by anthracene. This fraction was determined from the initial optical spectra. A set of experimental data was used to obtain the following ratio

$$\frac{\epsilon_{\text{ANT}}}{\epsilon_{\text{TPN}}} = 5.1 \pm 0.8 \quad (6)$$

Strictly speaking, eq 6 determines the lower limit for ϵ_{TPN} , because the reaction of energy transfer can compete with the process of radiationless TPN deactivation upon collision of this molecule with anthracene



It is, however, worth noting that at a large rate constant of energy transfer ($k_{\text{TE}} \approx k_{\text{diff}}$), the rate constant of radiationless deactivation is close to zero for many similar systems.^{35,36}

Comparing the yield of T–T absorption upon pulse photolysis for solutions of TPN and anthracene (Figure 8), the following equation was obtained

$$\frac{\epsilon_{\text{ANT}}\varphi_{\text{ANT}}}{\epsilon_{\text{TPN}}\varphi_{\text{TPN}}} = 28.1 \pm 0.7 \quad (8)$$

This equation makes it possible to estimate (at known $\epsilon_{\text{ANT}}/\epsilon_{\text{TPN}}$) the ratio between the quantum yields

$$\frac{\varphi_{\text{TPN}}}{\varphi_{\text{ANT}}} = 0.18 \pm 0.03 \quad (9)$$

For anthracene, the quantum yield of the triplet state (φ_{ANT}), the position of the T–T absorption band ($\lambda_{\text{T}}^{\text{max}}$), and its absorption coefficient (ϵ_{T}) depend on a solvent. Table 2 summarizes these values obtained for some solvents. Following this table, the position of the T–T absorption band of anthracene in hexane ($\lambda_{\text{T}}^{\text{max}} = 421 \text{ nm}$) almost coincides with this parameter for cyclohexane. Therefore, when determining φ_{TPN} and ϵ_{TPN} for TPN in hexane (eqs 6 and 9), the φ_{ANT} and ϵ_{ANT} values for anthracene in cyclohexane were used as standards.³⁵ Thus, when determining the parameters of GNB photochemical dissociation, for TPN below we use the values $\varphi_{\text{TPN}} = 0.13 \pm 0.02$ and $\epsilon_{\text{TPN}}(421 \text{ nm}) = 12\,700 \pm 2000 \text{ M}^{-1}\text{cm}^{-1}$. The TPN T–T absorption spectrum (Figure 4) can be used to determine the absorption coefficient at other wavelengths.

TABLE 3: Position of Maxima and the Molar Absorption Coefficients of the Absorption Bands of Stable and Unstable Germynes

germylene	solvent	λ_{\max} (nm)	ϵ (M ⁻¹ cm ⁻¹)	ref
Stable Germynes				
[2,4,6-(CF ₃) ₃ C ₆ H ₂] ₂ Ge:	hexane	374	1300	36
Tb(Mes) ₃ Ge:	hexane	575	1600	37, 38
(CH(SiMe ₃) ₂) ₂ Ge:	hexane	414	970	39, 40
[Mes*] ₂ Ge:	hexane, THF ^a	430	520	41
((Me ₃ Si) ₂ CCH ₂) ₂ Ge:	hexane, THF ^a	450	320	42
(But ₂ N) ₂ Ge:	cyclohexane	445	420	43
Unstable Germynes				
(Ph ₂) ₂ Ge:	hexane	500	1650	44
Mes ₂ Ge:	hexane	550	1440	44

^a THF = tetrahydrofuran.

3.5. Parameters of Photocleavage of GNB. The above ϵ_{TPN} value is used to calculate a relative yield of TPN in the triplet state upon excitation of GNB. The amplitude and kinetics of a change in optical density at 315 nm after the laser pulse (Figure 3) were determined by both the TPN absorption in the ground, excited, and triplet states and the disappearance of GNB absorption. The ratio between the additional absorption, just after the pulse (A_0) and at long times (D_∞) when the triplet TPN state has relaxed into the ground singlet state of this molecule, follow the equation:

$$\frac{A_0}{D_\infty} = \left(1 + \frac{\epsilon_T - \epsilon_G}{\epsilon_S - \epsilon_G} \frac{[T_1]}{[S_0]}\right) \left(1 + \frac{[T_1]}{[S_0]}\right) \quad (10)$$

where $\epsilon_T = \epsilon_{\text{TPN}}$, ϵ_S , and ϵ_G are the absorption coefficients of the TPN T–T absorption, its absorption in the ground singlet state, and the absorption of GNB at 315 nm, $[T_1]$ and $[S_0]$ are the yields (concentrations) of TPN in the excited triplet (T_1) and ground singlet (S_0) states upon GNB molecule photodissociation. All three absorption coefficients are known, and the A_0/D_∞ ratio can be found from the kinetic curves. Therefore, eq 10 can be used to estimate the $[T_1]/[S_0]$ ratio.

The treatment of kinetic curves at 315 nm (one is shown in Figure 3) provides $A_0/D_\infty = 1.45 \pm 0.1$. Substituting A_0/D_∞ and $(\epsilon_T - \epsilon_G)/(\epsilon_S - \epsilon_G) = 2.34 \pm 0.1$ into eq 10 indicates that $[T_1]/[S_0] = \gamma_{T_1}/\gamma_{S_0} = 0.51 \pm 0.1$ (where γ_{T_1} and γ_{S_0} are the relative yields of the triplet and ground singlet states of TPN). Because the total TPN yield per one GNB molecule equals unity ($\gamma_{T_1} + \gamma_{S_0} = 1$), then $\gamma_{T_1} = 0.34 \pm 0.04$ and $\gamma_{S_0} = 0.66 \pm 0.07$.

Upon GNB photodissociation, the final product (TPN molecule) can be in the ground (S_0), triplet (T_1), and singlet (S_1) excited states.²⁰ The quantum yield and the lifetime of fluorescence from the S_1 state are $\tau_f \approx 3$ ns and $\varphi_f = 0.09$ for TPN in methylcyclohexane at 297 K.²⁰ As shown previously, the quantum yield of the triplet state $\varphi_T = 0.13 \pm 0.02$, therefore, the excited TPN molecule effectively relaxes into the ground state as a result of radiationless processes ($\varphi_{\text{nonirr}} = 1 - \varphi_f - \varphi_T \approx 0.79$). Thus, the value $\gamma_{S_0} = 0.66 \pm 0.07$ can be determined by both the direct appearance of TPN in the ground state and either the radiation or the radiationless relaxation of the excited state S_1 ($S_1 \rightarrow S_0$). The parameter $\gamma_{T_1} = 0.34 \pm 0.04$ can also be determined by both the direct formation of the triplet state and the intersystem crossing $S_1 \rightarrow T_1$. If to indicate the relative populations of S_1 , T_1 , and S_0 states of TPN after the GNB photodissociation as x , y , and z ($x + y + z = 1$), respectively, it is possible to write the equation

$$y = \gamma_{T_1} - \frac{\varphi_T}{1 - \varphi_T} (\gamma_{S_0} - z) \quad (11)$$

So, if $z = 0$ (the population of ground S_0 state is zero), the

substitution of φ_T , γ_{T_1} , and γ_{S_0} to eq 11 gives $y = 0.24 \pm 0.06$. In another extreme case at $x = 0$ (the population of excited S_1 state is zero), $y = \gamma_{T_1} = 0.34 \pm 0.04$ ($z = \gamma_{S_0} = 0.66 \pm 0.07$). Thus, the direct yield of the triplet state of TPN upon GNB photodissociation can vary over the range 0.24–0.34. It is worth noting that, because of a small quantum yield of intersystem crossing ($\varphi_T = 0.13$), only the S_1 state fails to give rise to a substantial number of TPN molecules in the triplet state ($\gamma_{T_1} = 0.34$).

The obtained values of the T_1 state yield allow us to estimate the absorption coefficient of dimethylgermylene absorption band (Figure 2), which is observed as a fast component in the kinetic curves (Figure 3). In this case, the molar absorption is of the form

$$\epsilon_{\text{Me}_2\text{Ge}} = \epsilon_{\text{TPN}} \frac{A_1}{A_2} \gamma_{T_1} \quad (12)$$

where A_1 and A_2 are the amplitudes of the fast and slow components. Using the data in Figure 2, we get the value $\epsilon_{\text{Me}_2\text{Ge}} \approx 2400 \pm 500 \text{ M}^{-1}\text{cm}^{-1}$.

Table 1 summarize the positions of the maxima of dimethylgermylene absorption bands in frozen matrices and solutions. However, the absorption coefficient of these bands is still unknown. The optical absorption bands of germynes are determined by electron transfer from the binding orbital $2a_1$ (linear combination of $4s$ and $4p_z$ orbitals of Ge and of σ orbitals of ligands X in germylene $X_2\text{Ge}$) to the nonbonding orbital $1b_1$ (the C_{2v} symmetry group), which is the $4p_y$ orbital of the Ge atom. Transition between the terms, $^1A_1 \rightarrow ^1B_1$, is resolved with respect to symmetry. However, location of the orbitals in different planes reduces both their overlapping and their transition intensity. Thus, the absorption coefficient should be 1–2 orders of magnitude as small as the highest value of $\sim 10^5 \text{ M}^{-1}\text{cm}^{-1}$. For stable germynes, the bands do have the small values of about $10^3 \text{ M}^{-1}\text{cm}^{-1}$ (Table 3).

In a recent paper,⁴⁴ the absorption coefficients were determined for some unstable germynes (Table 3) that also vary over this range. Thus, the above estimate of the dimethylgermylene absorption coefficient is in fair agreement with the literature data on other germynes.

The recombination of dimethylgermylene leads to the tetramethyldigermene appearance, which has the absorption band with a 370 nm maximum (see additional band with 370 nm in spectrum of A_2 component in Figure 4). The ratio of optical densities of absorption bands of these species (spectrum of fast component A_1 in Figure 2 for dimethylgermylene) allows for an estimate of the molar absorption for tetramethyldigermene ($\epsilon_{\text{Me}_2\text{Ge}-\text{GeMe}_2} \approx 3600 \pm 800 \text{ M}^{-1}\text{cm}^{-1}$). The tetramethyldigermene is also the transient particle and disappears in the

reaction of dimerization with rate constants ($2k/\epsilon = (4.8 - 0.65) \times 10^6 \text{ cm s}^{-1}$),^{5,14,45} with the formation of oligogermanes. Taking into account the absorption coefficient, the bimolecular rate constant will be equal to $2k = 1.7 \times 10^9 - 2.3 \times 10^8 \text{ M}^{-1}\text{s}^{-1}$. The observed rate constant of tetramethyldigermene decay is $k_{\text{obs}} = 2kC = 2k\Delta D/\epsilon l \approx (2.0 - 0.3) \times 10^5 \text{ s}^{-1}$ (C is the concentration of tetramethyldigermene and ΔD is its optical density at 370 nm). Thus, its decay rate is essentially less than the decay of ^1TPN ($k_{\text{obs}} = 4.6 \times 10^5 \text{ s}^{-1}$).

3.6. Discussion of Results. As shown above, the considerable portion of triplet TPN state (70 – 100%) can arise directly (without intermediate S_1 state) from GNB photodissociation. In previous studies,²⁰ there are no qualitative estimates of the yield of various TPN states, because the authors did not determine the absorption coefficient of the T–T absorption of this molecule. Therefore, they assumed that the triplet state results only from the intersystem crossing in TPN, ($S_1 \rightarrow T_1$). This assumption accounts for the absence of the chemical polarization of ^1H nuclei on TPN and GNB under irradiation. As a result, it was concluded²⁰ that dimethylgermylene is formed though a one-step mechanism upon a synchronous break of two Ge–C bonds.

It is worth noting that the TPN molecule in the triplet state can arise from GNB photodissociation from the triplet state (^3GNB). However, the previous studies²⁰ have assumed that this mechanism is not realized, because in the sensitized photolysis (triplet sensitizers—benzophenone and xanthone) there is no intermediate absorption that could be assigned to the triplet GNB state. As compared with germanorbornadiene, for TPN, the process of the triplet–triplet energy transfer from sensitizers is effective enough. Indeed, the absolute absence of photoreaction from the ^3GNB state is not guaranteed, because the intersystem crossing ($S_1 \rightarrow T_1$) in this molecule and the triplet–triplet energy transfer between two molecules are two different processes. The absence of one of these does not guarantee the absence of the other.

Assuming the GNB photodissociation occurs in the singlet state, then the appearance of the triplet TPN state can be assigned only to the formation of the $\text{TPN}^*\cdots\text{GeMe}_2$ biradical in which one Ge–C band is broken and can evolve from the initial singlet state into the triplet state. In this case, upon the decay of the triplet biradical (the break of the second Ge–C bond) one of the partners (Me_2Ge or TPN) could be in the triplet state. Analyzing the signs of the ^1H CIDNP effects upon GNB photolysis in the presence of acceptors indicates that dimethylgermylene can arise in the triplet state.^{21,22,46} Unfortunately, the CIDNP method fails to provide quantitative estimates, and the relative yield of Me_2Ge^T remains unknown. Our data indicate that a relative yield of the triplet state of dimethylgermylene varies over the range of 0–66%. The lower limit (0%) can be realized in the case of the dissociation of the triplet state of the biradical $\text{TPN}^*\cdots\text{GeMe}_2$, with the appearance of TPN only in the triplet state. This is hardly probable, because CIDNP confirms the existence of dimethylgermylene in the triplet state.^{21,22,46} The upper limit of the yield of the triplet Me_2Ge restricts itself to $\gamma_{\text{Me}_2\text{Ge}} = 1 - \gamma_{\text{TPN}} = 0.66$.

The data set obtained by the methods of laser pulse photolysis and CIDNP indicates that the GNB photodissociation and the appearance of dimethylgermylene might be a result from several competing reactions. The primary process is the excitation of GNB into the first excited singlet state



Because the quantum yield of GNB photodissociation is

substantially smaller than unity ($\varphi \approx 0.4$)²⁰ and fluorescence is actually absent, the major mechanism of excited singlet state decay for this molecule is the radiationless relaxation into the ground state. From the excited state, ^1GNB can dissociate to break two Ge–C bonds and form TPN and dimethylgermylene. The TPN molecule could be in either the ground or the excited singlet state



A long-wave GNB absorption band is localized in the range of 275 nm, which corresponds to an energy of absorbed quantum of about 4.5 eV. The effective thermal decomposition of GNB at about 100 °C^{16,47} indicates that the energy of the first Ge–C bond break is about 1.0–1.2 eV⁴⁸ (the break of the second Ge–C bond will require a much smaller amount of energy). About 3.3–3.5 eV can be spent to form the excited ^1TFN molecule, which is insufficient because a maximum of the long-wave TPN absorption band is at 300 nm (4.1 eV). Therefore, the reaction (15) is improbable.

The appearance of one of the partners (TPN or Me_2Ge) in the triplet state upon ^1GNB dissociation is forbidden by the rule of total spin conservation. This rule does not forbid a parallel formation of two particles in the triplet states



However, the probability of such a process is much smaller (1/9) than the probability of particle appearance in singlet states (eq 14), and in this case, there is an energy problem, because a reserve of 3.2–3.5 eV is insufficient for the simultaneous appearance of ^1TPN (2.45 eV) and $^T\text{GeMe}_2$ (1.2 eV)^{49–51} particles.

The processes where the GNB photodissociation occurs in one act with the break of both of the Ge–C bonds have been described previously. It is most probable that the reaction in eq 14 will occur in which the final products arise in the ground singlet states. Assumption of a single act means that a time interval between the breaks of the first and second Ge–C bonds is much shorter than the time resolution of the method of registration, and a short lifetime of the biradical (the break of the first bond)



fails to cause a substantial change in the yield of final products, including a change in the electron state of these products. However, the observation of CIDNP effects^{21,22,46} indicates that the lifetime of the biradical is sufficient for transition into the triplet state.



From this state, the biradical can dissociate to give rise to one of the partners in the triplet state.



So, in various electron states, the final TPN molecule can arise in four reactions (eqs 14, 15, 19, and 20). A relative fraction of each channel is undetermined, and only the value

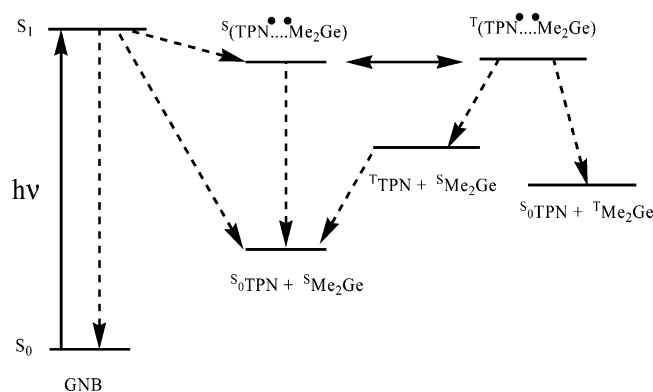


Figure 9. Diagram of the possible processes on GNB excitation.

$\gamma_{T_1} = 0.34$ indicates that the dissociation of the biradical (eq 19) determines almost one-third of the total yield of photoreaction. The detection of photo CIDNP effects in reactions of triplet dimethylgermylene^{20–22} points to the existence of the reaction in eq 20, but the yield of the triplet state is not defined.

The absence of the quantitative measurements of the product yield leads to the different conclusions about the mechanism of GNB phototransformations. Figure 9 gives a qualitative scheme of possible photophysical and photochemical processes for GNB. The probabilities of the realization of all processes can be calculated by determining a relative yield of dimethylgermylene in the triplet state.

4. Conclusions

Laser pulse photolysis was used to consider the primary processes of germanorbornadiene phototransformation. The absorption coefficient of T–T absorption and the quantum yield of the intercombination conversion of tetraphenylanthracene were determined using the method of triplet–triplet energy transfer. The data was used for the estimating the relative yield of the triplet TPN state upon germanorbornadiene photodissociation. It has been shown that the intercombination conversion ($S_1 \rightarrow T_1$) in the TPN molecule fails to provide the experimental yield of the TPN triplet. Thus, this state is likely to arise from the dissociation of the Ge–C bond in the biradical that initially forms in the singlet state and then evolves into the triplet state. This conclusion is in fair agreement with the earlier observation^{21,22} of CIDNP effects on both the initial GNB and the product of dimethylgermylene, which could also be in the triplet state.

Acknowledgment. This work was supported by the Russian Foundation for Fundamental Research (Grants RFFR 05-03-32474, 03-03-33134, 03-03-39008GFEN, and 04-03-32277), the Ministry of Education of RF “Universities of Russia” (Grant UR.05.01.020), and the INTAS Fellowship Grant for Young Scientists (Grant 03-55-1472).

References and Notes

- Barrau, J.; Escudié, J.; Satgé, J. *Chem. Rev.* **1990**, *90*, 283.
- Neumann, W. P. *Chem. Rev.* **1991**, *91*, 311.
- Wakasa, M.; Yoneda, I.; Mochida, K. *J. Organomet. Chem.* **1989**, *366*, C1.
- Mochida, K.; Yoneda, I.; Wakasa, M. *J. Organomet. Chem.* **1990**, *399*, 53.
- Mochida, K.; Kano, N.; Kato, R.; Kotani, M.; Yamauchi, S.; Wakasa, M.; Hayashi, H. *J. Organomet. Chem.* **1991**, *415*, 191.
- Mochida, K.; Ginyama, H.; Takahashi, M.; Kira, M. *J. Organomet. Chem.* **1998**, *553*, 163.
- Mochida, K.; Tokura, S.; Murata, S. *Chem. Commun.* **1992**, 250.
- Bobbins, K. L.; Maloney, V. M.; Gaspar, P. P. *Organometallics* **1991**, *10*, 2772.
- Barrau, J.; Bean, D. L.; Welsh, K. M.; West, R.; Michl, J. *Organometallics* **1989**, *8*, 2606.
- Tomoda, S.; Shimoda, M.; Takeuchi, Y.; Kajii, Y.; Obi, K.; Tanaka, I.; Honda, K. *Chem. Commun.* **1988**, 910.
- Ando, W.; Tsumuraya, T.; Sekiguchi, A. *Chem. Lett.* **1987**, 317.
- Ando, W.; Itoh, H.; Tsumuraya, T. *Organometallics* **1989**, *8*, 2759.
- Sakurai, H.; Sakamoto, K.; Kira, M. *Chem. Lett.* **1984**, 1379.
- Mochida, K.; Tokura, S. *Bull. Chem. Soc. Jpn.* **1992**, *65*, 1642.
- Bleckmann, P.; Minkwitz, R.; Neumann, W. P.; Schriewer, M.; Thibud, M.; Watta, B. *Tetrahedron Lett.* **1984**, *25*, 2467.
- Kocher, J.; Lehnig, M.; Neumann, W. P. *Organometallics* **1988**, *7*, 1201.
- Neumann, W. P.; Schriewer, M. *Tetrahedron Lett.* **1980**, *21*, 3273.
- Billeb, G.; Neumann, W. P.; Steinhoff, G. *Tetrahedron Lett.* **1988**, *29*, 5245.
- Schriewer, M.; Neumann, W. P. *J. Am. Chem. Soc.* **1983**, *105*, 897.
- Görner, H.; Lehnig, M.; Weisbeck, M. *J. Photochem. Photobiol., A* **1996**, *94*, 157.
- Egorov, M. P.; Ezhova, M. B.; Kolesnikov, S. P.; Nefedov, O. M.; Taraban, M. B.; Kruppa, A. I.; Leshina, T. V. *Mendeleev Commun.* **1991**, *1*, 143.
- Kolesnikov, S. P.; Egorov, M. P.; Galminas, A. M.; Ezhova, M. B.; Nefedov, O. M.; Leshina, T. V.; Taraban, M. B.; Kruppa, A. I.; Maryasova, V. I. *J. Organomet. Chem.* **1990**, *391*, C1.
- Grivin, V. P.; Plyusnin, V. F.; Khmelinski, I. V.; Bazhin, N. M.; Mitewa, M.; Bontchev, P. R. *J. Photochem. Photobiol., A* **1990**, *51*, 371.
- Compton, R. H.; Grattan, T. V.; Morrow, T. *J. Photochem.* **1980**, *14*, 61.
- Carmichael, I.; Helman, W. P.; Hug, G. L. *J. Phys. Chem. Ref. Data.* **1987**, *16*, 239.
- Brinen, J. S.; Orloff, M. K. *J. Chem. Phys.* **1969**, *51*, 527.
- Kolesnikov, S. P.; Egorov, M. P.; Dvornikov, A. S.; Kuz'min, V. A.; Nefedov, O. M. *Metalloorg. Khim.* **1989**, *2*, 799 (in Russian).
- Mochida, K.; Kikkawa, H.; Nakadaira, Y. *J. Organomet. Chem.* **1991**, *412*, 9.
- Mochida, K.; Wakasa, M.; Nakadaira, Y.; Sakaguchi, Y.; Hayashi, H. *Organometallics* **1988**, *7*, 1869.
- Mochida, K.; Ginyama, H.; Takahashi, M.; Kira, M. *J. Organomet. Chem.* **1998**, *553*, 163.
- Porter, G.; Windsor, M. W. *Proc. R. Soc. London, Ser. A* **1958**, *245*, 238.
- Kavashima, Y.; Hashimoto, H.; Nakano, H.; Hirao, K. *Theor. Chem. Acc.* **1999**, *102*, 49.
- Bonneau, R.; Carmichael, I.; Hug, G. L. *Pure Appl. Chem.* **1991**, *83*, 289.
- Greiner, G. *J. Photochem. Photobiol., A* **2000**, *137*, 1.
- Nielsen, B. R.; Jorgensen, K.; Skibsted, L. H. *J. Photochem. Photobiol., A* **1998**, *112*, 127.
- Bender, J. E., IV; Banaszak Holl, M. M.; Kampf, J. W. *Organometallics* **1997**, *16*, 2743.
- Tokitoh, N.; Kishikawa, K.; Okazaki, R.; Ssamori, T.; Nakata, N.; Takeda, N. *Polyhedron* **2002**, *21*, 563.
- Kishikawa, K.; Tokitoh, N.; Okazaki, R. *Chem. Lett.* **1998**, 239.
- Davidson, P. J.; Harris, D. H.; Lappert, M. F. *J. Chem. Soc., Dalton Trans.* **1976**, 2268.
- Goldberg, D. E.; Harris, D. H.; Lappert, M. F.; Tomas, K. M. *J. Chem. Soc., Dalton Trans.* **1976**, 945.
- Jutzi, P.; Schmidt, H.; Neumann, B.; Stämmler, H. G. *Organometallics* **1996**, *15*, 741.
- Kira, M.; Ishida, S.; Iwamoto, T.; Ichinohe, M.; Kabuto, C.; Ignatovich, L.; Sakurai, H. *Chem. Lett.* **1999**, 263.
- Lappert, M. F.; Slade, M. J. *J. Chem. Soc., Dalton Trans.* **1980**, 621.
- Leigh, W. J.; Harrington, C. R.; Vargas-Baca, I. *J. Am. Chem. Soc.* **2004**, *126*, 16105.
- Mochida, K.; Kayamori, T.; Wakasa, M.; Hayashi, H.; Egorov, M. P. *Organometallics* **2000**, *19*, 3379.
- Leshina, T. V.; Volkova, O. S.; Taraban, M. B. *Izv. Ross. Akad. Nauk, Ser. Khim.* **2001**, 1830 (in Russian).
- Kocher, J.; Lehnig, M. *Organometallics* **1984**, *3*, 937.
- Shusterman, A. J.; Landrum, B. E.; Miller, R. L. *Organometallics* **1989**, *8*, 1851.
- Su, M. D.; Chu, S. Y. *J. Am. Chem. Soc.* **1999**, *121*, 4229.
- Su, M. D.; Chu, S. Y. *J. Am. Chem. Soc.* **1999**, *121*, 11478.
- Su, M. D.; Chu, S. Y. *J. Phys. Chem. A* **1999**, *103*, 11011.